



# The University of Bradford Institutional Repository

<http://bradscholars.brad.ac.uk>

This work is made available online in accordance with publisher policies. Please refer to the repository record for this item and our Policy Document available from the repository home page for further information.

To see the final version of this work please visit the publisher's website. Access to the published online version may require a subscription.

**Link to publisher version:** <https://doi.org/10.1109/TCE.2017.014753>

**Citation:** Ali N, Almahainy R, Al-Shabli A et al (2017) Analysis of improved  $\mu$ -law companding technique for OFDM systems. IEEE Transactions on Consumer Electronics. 63(2): 126-134.

**Copyright statement:** © 2017 IEEE. Personal use of this material is permitted. Permission from IEEE must be obtained for all other uses, in any current or future media, including reprinting/republishing this material for advertising or promotional purposes, creating new collective works, for resale or redistribution to servers or lists, or reuse of any copyrighted component of this work in other works.

# Analysis of Improved $\mu$ -Law Compressing Technique for OFDM Systems

Nazar Ali, *Senior Member, IEEE*, Rola Almahainy, Abdullah Al-Shabli, *Student Members, IEEE*,  
Nawaf Almoosa, Raed Abd-Alhameed, *Senior Members, IEEE*

**Abstract**—High Peak-to-Average-Power Ratio (PAPR) of transmitted signals is a common problem in broadband telecommunication systems using an orthogonal frequency division multiplexing (OFDM) modulation scheme, as it increases transmitter power consumption. In consumer applications where it impacts mobile terminal battery life and infrastructure running costs, this is a major factor in customer satisfaction. Compressing techniques have been recently used to alleviate this high PAPR. In this paper, a compressing scheme with an offset, amidst two nonlinear compressing levels, is proposed to achieve better PAPR reduction while maintaining an acceptable bit error rate (BER) level, resulting in electronic products of higher power efficiency. Study cases have included the effect of compressing on the OFDM signal with and without an offset. A novel closed-form approximation for the BER of the proposed compressing scheme is also presented, and its accuracy is compared against simulation results. A method for choosing best compressing parameters is presented based on contour plots. Practical emulation of a real time OFDM-based system has been implemented and evaluated using a Field Programmable Gate Array (FPGA).

**Index Terms**—Orthogonal frequency division multiplexing (OFDM), compressing, PAPR reduction, Field Programmable Gate Array (FPGA).

## I. INTRODUCTION

Orthogonal Frequency Division Multiplexing (OFDM) is a firmly established modulation technique in modern broadband wired and wireless communication systems. Because of its robustness to multi-path fading and higher spectral efficiency, OFDM is currently implemented in a number of popular consumer electronics including mobile phones, WiFi-based electronic devices such as tablets, laptops, and their supporting wireless networks.

This work was supported in part by the Semiconductor Research Corporation (SRC), USA & Advanced Technology Investment Company (ATIC) – Abu Dhabi, UAE under Task ID: 2440-011.

N. Ali is with the Department of Electrical and Computer Engineering, Khalifa University, UAE (e-mail: n.ali@kustar.ac.ae).

R. Almahainy is with the Department of Electrical and Computer Engineering, Khalifa University, UAE (e-mail: rola.almahainy@kustar.ac.ae).

A. Al-Shabli is with the Department of Electrical and Computer Engineering, Khalifa University, UAE (e-mail: abdullaalshabli@gmail.com).

N. Almoosa is with the Department of Electrical and Computer Engineering, Khalifa University, UAE (e-mail: nawaf.almoosa@kustar.ac.ae).

R. Abd-Alhameed is with the University of Bradford, Bradford, U.K. (e-mail: r.a.a.abd@brad.ac.uk).

OFDM signals, however, have one critical drawback of high peak to average power ratio (PAPR) of around 12 dB [1]. This may cause in-band spectral growth and out-of-band radiation (spectral regrowth) if the power amplifier at the transmitter is operated to provide maximum DC/RF conversion efficiency.

In addition, high PAPR demands high dynamic range for the mixer, DAC (digital to analog converter) and ADC (Analog to digital Converter) blocks of the transceiver system. This adds extra constraints on the designer engineer and electronic industry alike, resulting in a more costly product.

Because of the enormous commercial growth in personal communications and as power amplifiers (PAs) consume about 25% of the handheld device power [1], improving the efficiency of the PA is considered a priority.

Many techniques have been proposed to reduce the PAPR of the OFDM systems including, clipping and filtering [2]-[3], coding [4]-[5], and multiple signal representation techniques [6]-[7] such as partial transmit scheme (PTS), etc. Nonlinear compressing transform schemes [8]-[12] are another attractive option due to their good performance and being easy to implement at the baseband level.

Compressing schemes compress larger amplitude signals and expand smaller ones, resulting in a lower PAPR. However, all compressing techniques are characterized as distorting methods due to their ability to corrupt the signal by limiting its envelope. They are also very sensitive to channel noise because of their inherent nonlinear characteristics.

Various compressing transforms have been proposed in literature to reduce PAPR.  $\mu$ -law compressing scheme has been originally proposed in speech signal processing [13]. Lower PAPR relaxes the linearity requirement of the PA resulting in a higher efficiency and hence, power saving. Normally the power saving is proportional to the compressing level. Unfortunately, since the opposite of what happens in the transmitter is implemented in the receiver, the effect of channel noise becomes more apparent and this causes the overall system Bit Error Rate (BER) to degrade, hence negating the PAPR improvement. The authors in [14] suggested a hyperbolic tangent (HT) function technique to reduce the PAPR. They addressed the issue of increased average power as a result of compressing and suggested a technique for normalizing it. Targeting the linearity trait, a novel linear non-symmetric transform (LNST) outperform

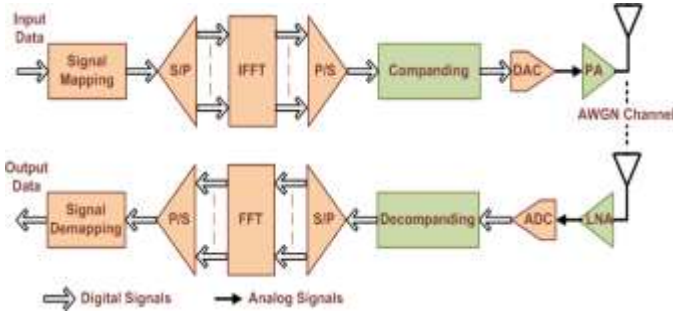


Fig. 1. OFDM baseband transceiver system model with companding blocks.

logarithmic-based transforms is proposed in [15]. The main idea is to treat large and small amplitudes of the OFDM signal as two independent parts with one inflexion point.

In the present paper, an improved two- $\mu$ S Companding Scheme (ITMs) is proposed to achieve better PAPR reduction than conventional companding schemes while maintaining an acceptable BER performance of the transceiver system. The idea of the proposed method is to expand the OFDM signal with two different  $\mu$ -values separated by a threshold while introducing an offset to cancel the resulting sharp step between the two companding levels. Simulation results show that better PAPR/BER tradeoff is achieved, as compared to the existing companding schemes. Also, unlike some other techniques, this scheme does not require additional system bandwidth.

Improving the signal PAPR with no additional system cost should invariably reduce the power consumption of electronic devices (transceiver systems) and the charging frequency of the battery-powered variety. This is true in the context of handheld electronic products and fixed infrastructures like base stations. Also reducing the power consumption of such widely spread electronics would ultimately have a positive impact on the environment.

In the following discussion, Section II details the OFDM transceiver baseband system and the proposed companding scheme. Section III discusses the selection of companding levels for better PAPR/BER tradeoff. Section IV compares the system performance for different companding schemes. Section V describes the mathematical analysis of the resulting bit error probability. Section VI shows an FPGA implementation of the proposed technique and section VII concludes the paper.

## II. SYSTEM STRUCTURE

Fig. 1 shows a typical block diagram for an OFDM based system. At the transmitter chain, the symbol mapping is a Quadrature Amplitude Modulation (QAM) and each symbol  $S_k$  in the I and Q parts of the constellation diagram has a distinctive amplitude and phase. The IFFT is applied to these symbols to generate OFDM symbol as follows

$$x(n) = \frac{1}{\sqrt{N}} \sum_{k=0}^{N-1} S_k e^{j \frac{2\pi}{N} kn}, \quad n = 0, 1, \dots, N-1 \quad (1)$$

where  $N$  is the number of subcarriers. In order to approximate the PAPR of the continuous OFDM signal, the discrete signal is oversampled. Oversampling by a factor of  $L$  is achieved by padding the symbols  $S_k$  with  $(L-1)N$  zeros. In this paper  $L=4$ . The PAPR of the discrete OFDM signal is stated as

$$PAPR = \frac{\max[|x(n)|^2]}{E[|x(n)|^2]} \quad (2)$$

where  $E[\cdot]$  denotes the expectation operator. The real and imaginary parts of  $x(n)$  are independent and each follows a Gaussian distribution with zero mean and variance  $\sigma^2 = E[|S_k|^2]/2$ .

Prior to transmission, the digital signal is companded then converted to the analog domain using a Digital-to-Analog (D/A) converter. The analog OFDM signal is transmitted over a time invariant Additive White Gaussian Noise (AWGN) channel. In the receiver, the opposite of the preceding will take place and the recovered output bits are the estimate of the input binary data bits.

In this work, a typical OFDM transceiver system is simulated to analyze the impact of the various companding schemes using the following specifications: 256 subcarriers, 1024-point IFFT/FFT and the randomly generated input data is modulated by 16QAM.

### A. $\mu$ -Law Companding.

The  $\mu$ -law companding scheme is a logarithmic-based nonlinear mechanism for PAPR reduction. In this technique, the small amplitudes of the signal are enlarged so the difference between the peaks and small values is reduced [13]. The mathematical formulation for the output of  $\mu$ -law companding and decompanding algorithms are  $D(x)$  and  $\bar{D}(r)$  respectively

$$D(x) = \frac{v}{\log(1+\mu)} \log\left(1 + \frac{\mu}{v}|x|\right) \text{sgn}(x) \quad (3)$$

$$\bar{D}(r) = \frac{v}{\mu} \left( e^{\frac{|r|\log(1+\mu)}{v}} - 1 \right) \quad (4)$$

where  $x$  is the baseband OFDM signal,  $r$  is the received signal after the channel,  $v$  is the maximum amplitude of the signal  $x$ ,  $\mu$  is the companding level and  $\text{sign}(\cdot)$  is the signum function. In the following analysis, the companding and decompanding functions, such as (3) and (4), are applied separately to the I and Q signals.

Fig. 2 shows the effect of varying  $\mu$  on both PAPR and BER. It is clear that at low  $\mu$  values, the PAPR decreases quite rapidly and then subsides at high values whilst the BER changes almost constantly with  $\mu$ . Therefore, it is clear for best results; small  $\mu$ -values should be targeted.

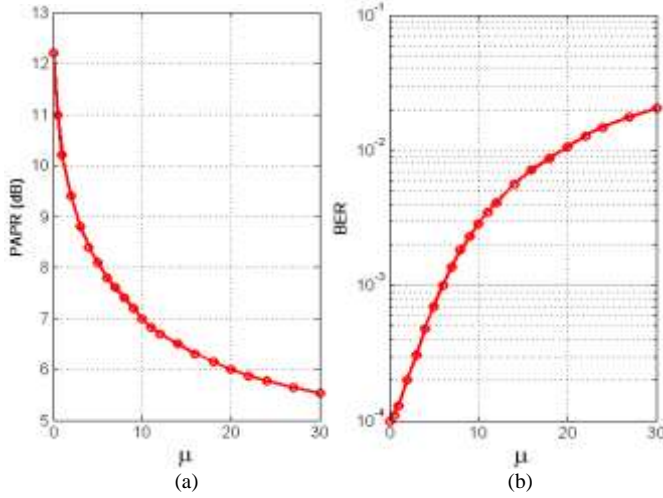


Fig. 2. (a) PAPR vs.  $\mu$  (b) BER vs.  $\mu$  at SNR = 15 dB: Illustration of the trade-off between decreasing PAPR and increasing BER as  $\mu$  increases.

### B. Two $\mu$ s-Companding

In this technique a threshold  $\alpha$  is introduced in the companding operation so that the signal is companded with  $\mu_1$  value below the threshold while  $\mu_2$  is applied to the rest as shown in Fig. 3(a). With this arrangement, the values of  $\mu$  and the threshold can be varied according to the system requirements for optimum PAPR and BER performances [16]. Although this is outside the scope of this paper, a practical implementation of such an adaptive operation would include a closed-loop feedback between the transmitter and receiver based on using the Error Vector Magnitude (EVM) proposed in [17] to evaluate the BER.

Typical results of system PAPR and BER values are shown in Figs. 3(b)-(c). From the simulation results, it was clear that the performance of this technique is better than the  $\mu$ -law companding regime in achieving better PAPR reduction with a tolerable BER or SNR increase. For this scheme, the best obtained values were  $\Delta\text{PAPR} = 3.3$  dB and  $\Delta\text{SNR} = 0.4$  dB at  $\mu_{1,2} = 3, 2$ , which yielded a net gain of 2.9 dB. This is better than  $\Delta\text{PAPR} = 3.3$  dB and  $\Delta\text{SNR} = 0.7$  dB at  $\mu = 3$ , resulting a net gain of 2.6 dB for the  $\mu$ -law. In the preceding,  $\Delta\text{PAPR}$  is the improvement or reduction in the PAPR while  $\Delta\text{SNR}$  is the increase in the SNR required to keep the BER constant at  $10^{-4}$  level.

The drawback, however, of the above two  $\mu$ s system is the introduction of the step. This makes the decompanding process at the receiver more complex, particularly when  $\mu_1 > \mu_2$  as illustrated in Fig. 3(a) (the solid red trace). Two values of the companded signal will appear as one value making it very difficult to distinguish between them at the receiver. Consequently, in order to recover the original signal successfully in a real-time system, additional information should accompany the transmitted data which results in a higher system bandwidth. In addition, the presence of a step in the companded and decompanded signals is highly undesirable, as this would distort the signal resulting in higher noise.

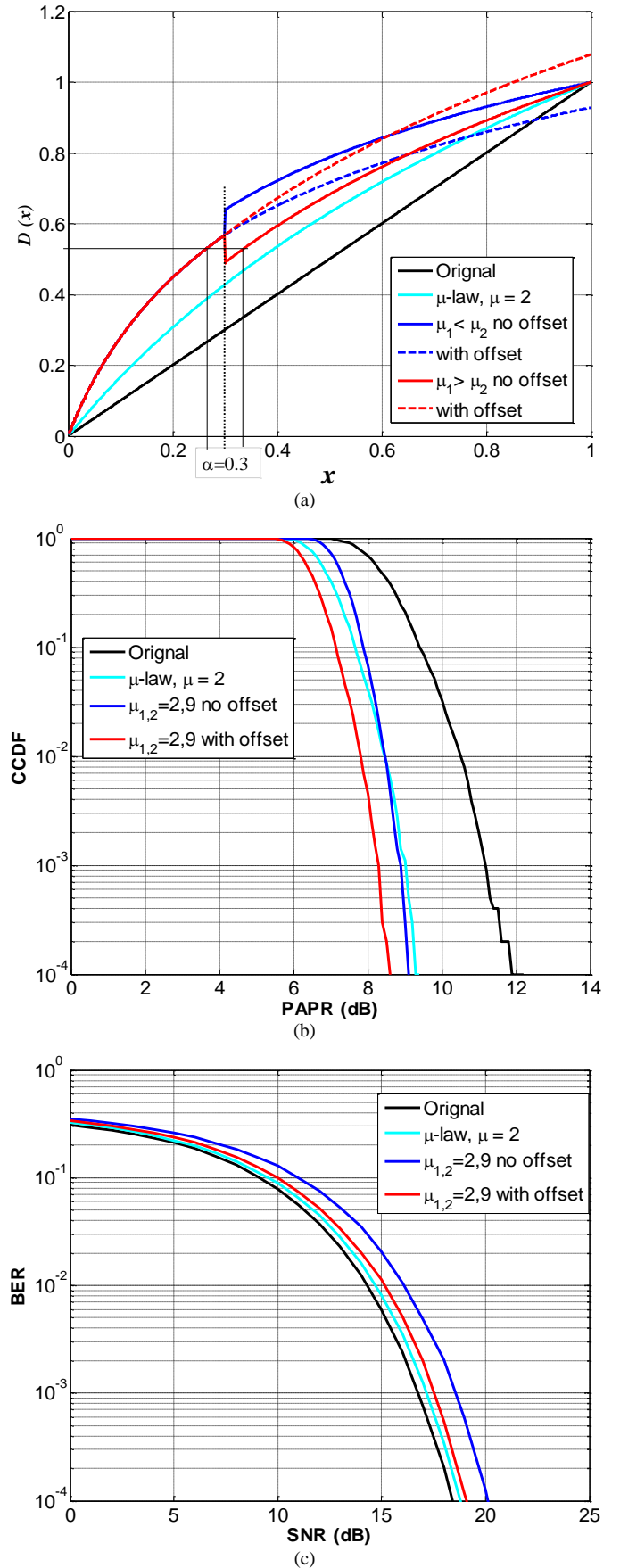


Fig. 3. (a) Various  $\mu$ -based companding profiles, (b) CCDF of PAPR, and (c) BER as a function of SNR.

### C. Proposed Scheme – Improved Two $\mu$ s-Companding

The idea of the proposed companding mechanism is to have an optimum tradeoff between lower PAPR and acceptable degradation in BER with ease of practical implementation.

In order to remedy the problems of the TMs scheme, the step at the threshold was eliminated by the introduction of an offset resulting in a smooth transition from  $\mu_1$  to  $\mu_2$ , Fig. 3(a). The red traces in Figs. 3(b)-(c) illustrate the impact of this idea on the PAPR and BER performances when applied to the TMs. It is clear that adding an offset has improved the PAPR and BER simultaneously.

The mathematical formulation for the output of the Improved Two  $\mu$ s (ITMs) companding and decompanding transforms are  $D_{ITM}(x, \mu_1, \mu_2)$  and  $\bar{D}_{ITM}(x, \mu_1, \mu_2)$  respectively, and can be expressed as

$$\begin{cases} D_1(x, \mu_1) = \frac{v}{\log(1 + \mu_1)} \log\left(1 + \frac{\mu_1 |x|}{v}\right) \text{sgn}(x), & |x| \leq \alpha \\ D_2(x, \mu_2) = \frac{v}{\log(1 + \mu_2)} \log\left(1 + \frac{\mu_2 |x|}{v}\right) \text{sgn}(x), & |x| > \alpha \end{cases} \quad (5)$$

$$\Delta = \min(D_2(x, \mu_2)) - \max(D_1(x, \mu_1)) \quad (6)$$

$$\therefore D_{ITM}(x, \mu_1, \mu_2) = \begin{cases} K(\mu_1, \mu_2) D_1(x, \mu_1), & |x| \leq \alpha \\ K(\mu_1, \mu_2) [D_2(x, \mu_2) - \Delta], & |x| > \alpha \end{cases} \quad (7)$$

$$\bar{D}_{ITM}(r, \mu_1, \mu_2) = \begin{cases} \frac{v}{K(\mu_1, \mu_2) \mu_1} \left[ e^{\frac{|r| \log(1 + \mu_1)}{v}} - 1 \right] \text{sgn}(r), & |r| \leq \beta \\ \frac{v}{K(\mu_1, \mu_2) \mu_2} \left[ e^{\frac{|r| \log(1 + \mu_2)}{v} |r + \Delta|} - 1 \right] \text{sgn}(r), & |r| > \beta \end{cases} \quad (8)$$

Applying companding increases the average power level of the OFDM signal in a form of data in the baseband processing [18]. In this work, the average powers of the companded and uncompanded signals were kept constant by using the normalization factor  $K(\mu_1, \mu_2)$  which simply equals the square root of the ratio of the two signal powers.

It should be emphasized that for the ITMs scheme to work efficiently  $\mu_1$  should be smaller than  $\mu_2$  so that removing the step would cause the peaks to compress resulting in a lower PAPR, Fig. 3(a). More details is offered in the next section.

In the next sections, further analysis is offered to validate the proposed scheme and to show a method of selecting best  $\mu_1$  and  $\mu_2$  values for optimum results.

### III. SELECTION OF $\mu_{1,2}$ FOR PAPR AND BER

An OFDM signal with a PAPR of around 12 dB has a signal voltage rms/peak ratio (SVPR) of 0.25. Therefore using a threshold of 0.3 would split the signal into two parts; one part where most of the signal around the average is subjected to  $\mu_1$ , and the second part with the peaks are expanded slightly or even compressed, in the case of ITMs, with  $\mu_2$ . Extensive simulation results using commercial software have confirmed this choice of threshold value.

Figs. 4(a)-(b) display contour plots of PAPR (in dB) for different  $\mu_1$ ,  $\mu_2$  and constant  $\alpha = 30\%$  of peak amplitude. These figures are the result of the companding at the transmitter only. Practical limits were selected in the analysis for  $\mu_{1,2} = 0-20$ . As  $\mu_1$  and  $\mu_2$  increase, PAPR decreases. Taking the diagonal line of  $\mu_1 = \mu_2$  and moving vertically or horizontally in the direction of higher  $\mu_1$  or  $\mu_2$ , it is clear that  $\mu_1$  has a much bigger effect on PAPR than  $\mu_2$ . This is apparent particularly in the case of the TMs scheme where the two  $\mu$ s are working independently as shown in Fig. 3(a). Fig. 4(a) also confirms that most of the signal is confined around and below the threshold. In Fig. 4(b), the two  $\mu$ s are working together to reduce the PAPR whereby  $\mu_1$  is mainly expanding the signal around the average leaving  $\mu_2$  to mostly expand or even compress the peaks when  $\mu_1 < \mu_2$ . Both figures show a stronger  $\mu_1$  dependency.

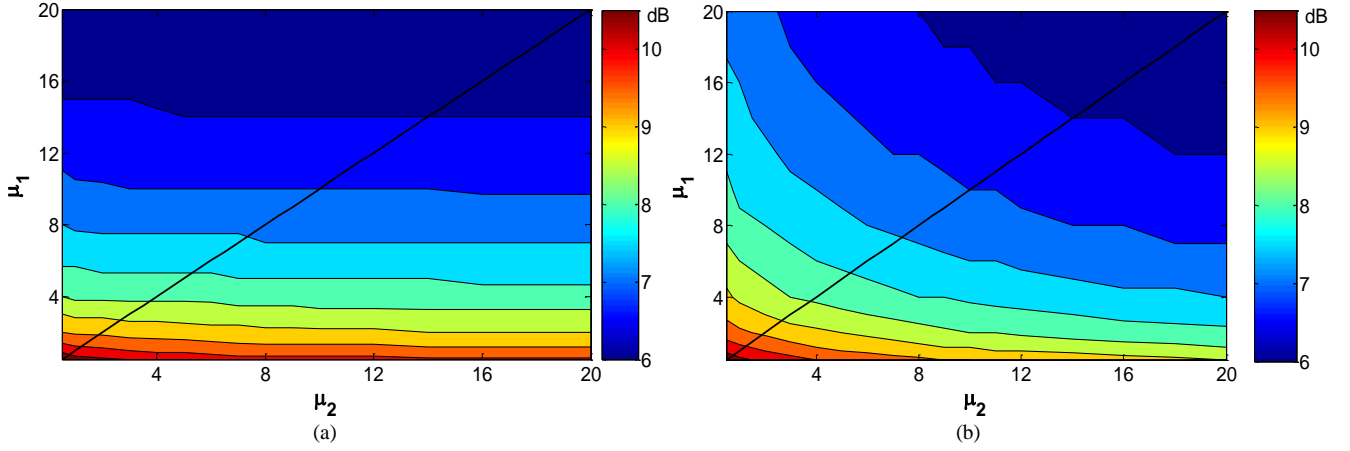
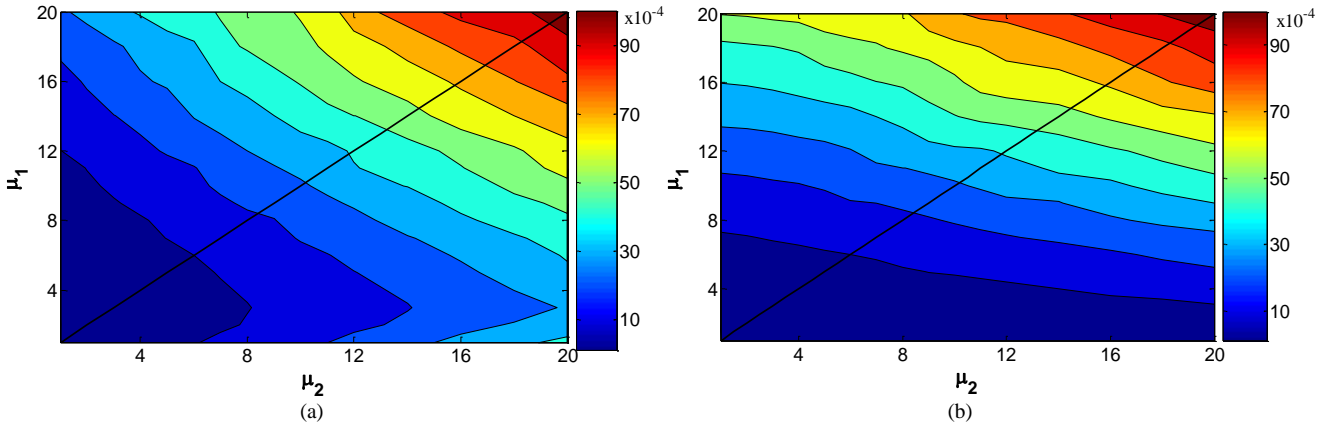
In Figs. 5(a)-(b), the BER is also plotted as a function of  $\mu_1$  and  $\mu_2$  for the same threshold and a fixed 15 dB SNR. Unlike the above, both figures are the result of the non-linearity of the compander at the transmitter and the decompander coupled with the channel noise at the receiver. For the most part, both plots show as  $\mu_1$  increases,  $\mu_2$  should decrease to keep the BER constant. Although  $\mu_1$  still has a larger effect than  $\mu_2$ , the fact that the companded signal arriving at the receiver is amplified, with a higher SVPR than 0.25 for the original signal, and the addition of channel noise, makes  $\mu_2$  has a bigger effect on the BER than on the PAPR for both, the TMs and ITMs regimes. However, in Fig. 5(a) for the TMs scheme, the opposite happens in the lower region, where  $\mu_1$  is much smaller than  $\mu_2$ . In this region, both  $\mu_1$  and  $\mu_2$  should increase or decrease together (constant step) to keep the BER constant. Since  $\mu_1$  is low, the effect of transmitter non-linearity is minimal, the primary cause of this behavior can be attributed to the size of the step occurring at the threshold between the two companding levels; as this step increases, its consequent signal distortion increases too, resulting in a higher BER.

Comparing Fig. 4(b) and Fig. 5(b), for the ITMs scheme, it is clear that in order to maximize PAPR gains,  $\mu_1$  should be greater than  $\mu_2$  and to have least BER deterioration  $\mu_2$  should be greater than  $\mu_1$ . Consequently, since low  $\mu$  values should be targeted, simulation results showed that the gains in keeping low BER and good PAPR reduction is best when  $\mu_2$  is greater than  $\mu_1$ .

### IV. COMPARISON WITH OTHER COMPANDING SCHEMES

Different classical companding schemes from the literature along with the proposed ITMs scheme are evaluated in the



Fig. 4. PAPR as a function of  $\mu_1$  and  $\mu_2$ , (a) without and (b) with offset.Fig. 5. BER as a function of  $\mu_1$  and  $\mu_2$  (SNR = 15 dB), (a) without and (b) with offset.

context of OFDM-based systems. Such techniques include the conventional  $\mu$ -law ( $\mu = 3$ ), the TMs ( $\mu_1 = 3$ ,  $\mu_2 = 2$ ,  $\alpha = 0.3$ ) and improved TMs ( $\mu_1 = 2$ ,  $\mu_2 = 7$ ,  $\alpha = 0.3$ ), hyperbolic tangent (HT) scheme ( $a = 0.4$  and  $b = 0.3$ ), and linear non-symmetric transform (LNST) with a scaling factor  $K = 0.5$ . Table I lists numerical results for different companding schemes in terms of PAPR reduction and additional (excess) SNR, in relations to the original (uncompanded) OFDM signal at constant BER level of  $10^{-4}$ .

The best PAPR reduction for the preceding cases is 7.73 dB achieved by hyperbolic tangent (HT) scheme but it results in an additional 11.2 dB SNR to keep BER constant. On the other hand, the best excess SNR is the one closest to the original OFDM signal, which is 0.4 dB for TMs scheme but the PAPR reduction performance is 3.3 dB. Also, the TMs scheme requires additional system bandwidth to recover the original signal. Yet, the ITMs produces better net gain (PAPR improvement-excess SNR) than the TMs scheme of 3.1 dB with no additional system requirements or complications.

TABLE I  
RESULTS OF SYSTEM PERFORMANCE FOR DIFFERENT SCHEMES

Companding Scheme	PAPR Reduction	Excess SNR	Net gain
$\mu$ -law @ $\mu=3$	3.3 dB	0.7 dB	2.6 dB

HT	7.73 dB	11.2 dB	-3.47 dB
LNST	3.23 dB	0.6 dB	2.63 dB
TM @ $\mu_{1,2}=3, 2$	3.3 dB	0.4 dB	2.9 dB
ITMs @ $\mu_{1,2}=2, 7$	3.7 dB	0.6 dB	3.1 dB

## V. MATHEMATICAL ANALYSIS OF ERROR PROBABILITY

A closed-form approximation for BER of improved TM companded OFDM signal is discussed in this section. The general BER expression for a conventional OFDM system utilizing a square signal constellation of MQAM modulation over the AWGN channel is defined in [19] as

$$P_e(\gamma_b) = \frac{4(\sqrt{M}-1)}{\sqrt{M} \ln M} Q\left(\sqrt{\frac{3 \ln M}{M-1}} \gamma_b\right) \quad (9)$$

where  $M$  is the modulation order,  $\gamma_b$  is the SNR per bit and  $Q(\cdot)$  is the  $Q$ -function given as

$$Q(x) = \int_x^\infty \frac{1}{\sqrt{2\pi}} \exp\left(-\frac{u^2}{2}\right) du \quad (10)$$

In the simulations of the system, and its practical realization as described below, the exponential function in (8) has been calculated accurately. To derive an analytical expression for BER, it is supposed instead that decompanding is performed using only the first two terms in the Taylor series of the exponential. Then, at the receiver end, letting  $S'_k$  denote the decision variable of the recovered data on the  $k^{\text{th}}$  subcarrier, this would be approximated after some mathematical simplifications as  $S'_k = \text{DFT}(\tilde{X})$ , where  $\tilde{X}$  is

$$\tilde{X} = \begin{cases} x + \omega_n \left( \frac{\log(1 + \mu_1)}{\mu_1 K} + \frac{x \log(1 + \mu_1)}{vK} \right), & |x| \leq \alpha \\ x + \omega_n \left( \frac{\log(1 + \mu_2)}{\mu_2 K} + \frac{x \log(1 + \mu_2)}{vK} \right), & |x| > \alpha \end{cases} \quad (11)$$

where  $\text{DFT}(\cdot)$  is the Discrete Fourier transform and  $\omega_n$  is the sampled AWGN signal. Note that  $S'_k$  is represented in accordance to the OFDM signal  $x$ . Consequently, the equivalent noise increment due to the proposed companding scheme (i.e., noise variance) is  $\sigma_{\text{ofTM}(1,2)}^2 = N_{\text{inc}} \sigma_{\omega}^2$  where  $N_{\text{inc}}$  is given as

$$N_{\text{inc}} = \begin{cases} \left( \frac{\log(1 + \mu_1)}{\mu_1 K} \right)^2 + \sigma_s^2 \left( \frac{\log(1 + \mu_1)}{vK} \right)^2, & |x| \leq \alpha \\ \left( \frac{\log(1 + \mu_2)}{\mu_2 K} \right)^2 + \sigma_s^2 \left( \frac{\log(1 + \mu_2)}{vK} \right)^2, & |x| > \alpha \end{cases} \quad (12)$$

where  $\sigma_{\omega}^2$  and  $\sigma_s^2$  are the original AWGN signal and OFDM signal variances. After substituting (12) in (9), the closed-form approximation of the BER in (15) is developed by taking the weighted-average of  $P_{e1}(\gamma_b)$  and  $P_{e2}(\gamma_b)$  in relation to the threshold and signal voltage rms/peak ratio (SVPR).

$$P_{e1}(\gamma_b) = \frac{4(\sqrt{M} - 1)}{\sqrt{M} \log_2 M} Q \left( \sqrt{\frac{3 \log_2 M}{M - 1} \frac{\gamma_b}{\sigma_{\text{ofTM}1}^2}} \right) \quad (13)$$

$$P_{e2}(\gamma_b) = \frac{4(\sqrt{M} - 1)}{\sqrt{M} \log_2 M} Q \left( \sqrt{\frac{3 \log_2 M}{M - 1} \frac{\gamma_b}{\sigma_{\text{ofTM}2}^2}} \right) \quad (14)$$

$$P_{\text{eITM}}(\gamma_b) = F(x; \sigma) P_{e1}(\gamma_b) + (1 - F(x; \sigma)) P_{e2}(\gamma_b) \quad (15)$$

where  $F(x; \sigma)$  is the cumulative distribution function of a Rayleigh distributed variable  $x$  (in this context the uncompanded signal amplitude) with a modal value of  $\sigma$ . Calculated for an OFDM signal with a PAPR  $\approx 12\text{dB}$ , the maximum voltage  $v$  is  $4\sigma$  and the threshold  $\alpha = 0.3$  corresponds to  $x = 1.2\sigma$ , yielding a weighting of  $1 - \exp(-0.72)$

$= 0.513$  for  $P_{e1}(\gamma_b)$  and  $0.487$  for  $P_{e2}(\gamma_b)$ .

Fig. 6 presents the behavior of the analytical and simulated BER for different companding levels  $\mu_1$  and  $\mu_2$ . It is clear that good matching is obtained up to values  $\mu_{1,2} \leq 20$ . This is due to the fact that the exponential function in the decompanded signal was approximated using only the first two terms of Taylor series expansion which is clearly insufficient when using higher companding levels. Including more terms of Taylor series expansion solves the issue but makes the

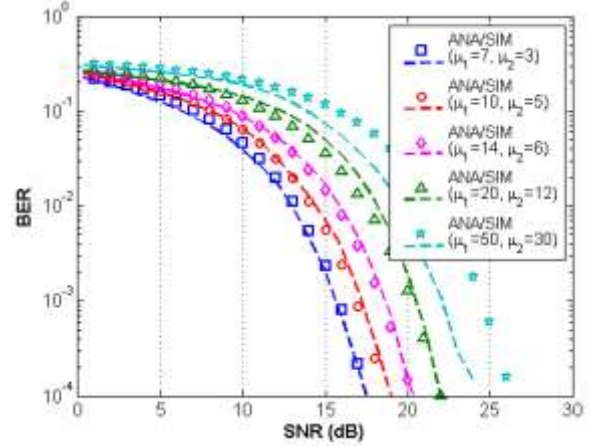


Fig. 6. Analytical and simulation results comparison for BER performance as a function of SNR.

analytical derivation much more complicated. Numerical approaches maybe used for higher  $\mu$  values but it is outside the scope of this paper and deemed unnecessary as best values of  $\mu_1$  and  $\mu_2$  are not higher than 10.

## VI. EXPERIMENTAL RESULTS

The OFDM-based system has been perceived by many as a digital transceiver system, therefore the performance can be analyzed sufficiently by simulation only. Such interpretation is inaccurate because the system is actually a mixture of analogue and digital components. Thus, hardware implementation on FPGA platform is an invaluable evaluation of the OFDM system performance in real-time.

### A. Hardware Testbed

A commercial FPGA hardware kit was used for implementation of the system. Fig. 7 demonstrates the top-level design model for the TMs companded OFDM system. The overall system is divided into several design paradigms, where each is built, simulated, analyzed and verified in both simulation and hardware. A typical OFDM transceiver system comprises the following: an input signal fed through the ADC and then goes through a P/S to up-sample the signal so that the output rate is 7-times faster. The in-phase and quadrature components are extracted from the incoming signal. The 16QAM data mapping is designed to give the required points for the constellation  $[-1 -1/3 \ 1/3 \ 1]$ . Its reciprocal operation is the 16QAM data demapping which is a simple comparator. The comparator output is the estimated real and imaginary

components that contribute to the output sine wave information. The FFT/IFFT operation is modeled by using Fast Fourier Transform (FFT) blocks.

The allocated system parameters for the companded OFDM transceiver model are 512-point IFFT/FFT, FPGA clock period of 80 ns and a 1Vpp analog input signal with a frequency of 10 kHz modulated by 16QAM scheme. The specified companding levels are  $\mu_1 = 10$ ,  $\mu_2 = 0$  and a threshold of 30% of peak amplitude. The radio channel is omitted so that the emphasis is placed on establishing proof of concept of the ITMs companding scheme in hardware.

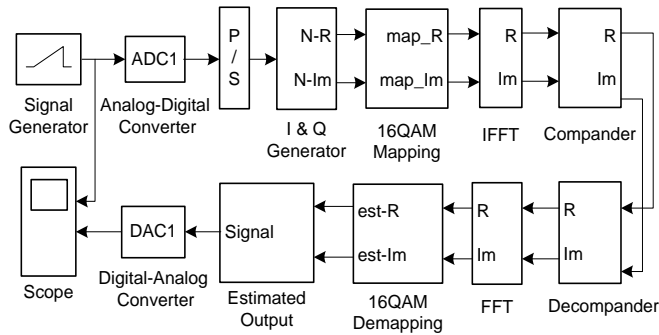


Fig. 7. Top-level design model for TMs companded OFDM transceiver.

### B. ITMs FPGA Implementation

The proposed Improved TMs algorithm, including companding and decompanding functions, was implemented as follows. Firstly, the incoming signal passes through the threshold design model to produce two sets of signals. Each set is companded using a different  $\mu$ -law value. The offset design model is then added to the second companded set to smoothen the abrupt transition. Subsequently, the two sets are summed to create the improved TMs companded signal in form of signed 2's comp. 28-bit fixed-point precision with 15 fractional bits.

In the  $\mu$ -law companding and decompanding design model, the natural logarithm is computed using a LOG block. Due to the lack of an exponential block, the exponential operation had to be designed completely in an equivalent manner using the first six terms of Taylor series expansion.

The overall proposed model is then added to the predesigned OFDM transceiver system. The cumulative delay at the Estimated Output Sinewave block is adjusted to match the overall delay and accurately re-generate the estimated sinewave information.

TABLE II  
DEVICE UTILIZATION SUMMARY

Resources	Resource Usage
Slices	4439 out of 15360 (28%)
LUTs	8,121 out of 30,720 (26%)
DSP48s	52 out of 192 (27%)
Bonded IOBs	62 out of 448 (13%)
RAMB16s	0 out of 192 (0%)

Table II illustrates the device utilization summary for improved TM companding and decompanding design model. The summary determines whether the system model fits the FPGA allocated resources. The proposed companding scheme

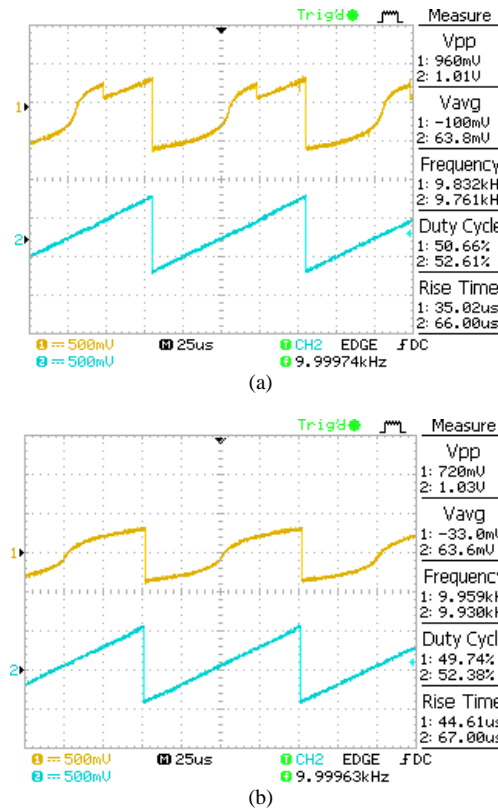


Fig. 8. Verification of the TMs companding scheme (a) without and (b) with offset. Trace 1) Companded sawtooth signal ( $\mu_1 = 10$ ,  $\mu_2 = 0$ ,  $\alpha = 0.3$ ), Trace 2) The input signal.

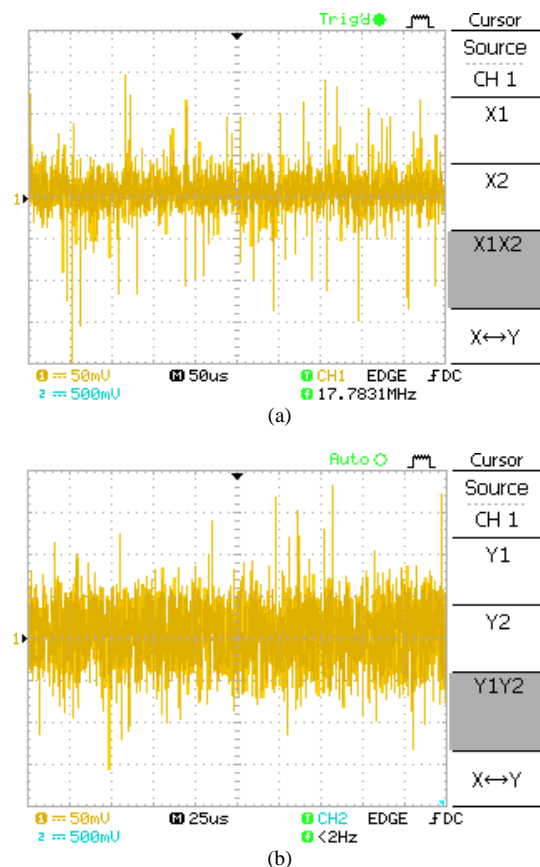


Fig. 9. Time domain representation of, (a) original OFDM signal, (b) companded OFDM signal.



was found to have a relatively low computational complexity in terms of hardware and therefore it required low processing power and time.

### C. Results

A real-time sawtooth analog signal is used for the initial testing of the Two- $\mu$ s companding system. In Fig. 8(a) signal amplitudes up to a threshold of 30% of the peak are companded with a  $\mu_1 = 10$  while the rest is left as is. Notice the effect of the TMs companding on the sawtooth shape in which the abrupt transition exists between the companded and uncompanded parts as expected. Introducing the offset amidst ( $\mu_1 = 10$ ,  $\mu_2 = 0$ ), however, will generate a continuous and smooth companded signal as depicted in Fig. 8(b). The output decompanded sawtooth signal has a clear uncorrupted shape. Therefore, the improved TMs companding and decompanding design model is working according to expectation. After integrating the proposed companding transform with the OFDM-based system model, the system performance is analyzed as follows. Fig. 9(a) and Fig. 9(b) present the time domain representation of the uncompanded and improved TMs companded OFDM signal respectively. The effect of companding is clearly observed on the OFDM signal envelope where the waveform has less amplitude variation compared to the original uncompanded signal.

TABLE III  
TABULATION OF PAPR RESULTS

System Model	Simulation	Hardware
Original OFDM	12.455 dB	12.6 dB
Improved TMs Companded OFDM	8.693 dB	9.107 dB

Table III shows PAPR comparison of simulation and hardware results for the original uncompanded and improved TMs companded OFDM signals, with  $\mu_1 = 10$ ,  $\mu_2 = 0$  and  $\alpha = 0.3$ . The numerical results obtained from the hardware implementation compare well with the simulation results with expected real-time errors. The sources of errors in the FPGA implementation may include timing, precision, quantization, overflow and rounding.

## VII. CONCLUSIONS

High PAPR of OFDM transmitted signals is a major drawback as it increases the power consumption of consumer electronic products and the infrastructure that supports them. Various techniques such as companding offer tradeoff between PAPR reduction and BER degradation. This tradeoff has been established by studying different versions of companding schemes. In this paper, amongst other companding schemes, the proposed Improved Two- $\mu$ s has been found to offer best reduction in the PAPR of 3.7 dB with a slight increase in the SNR of 0.4 dB yielding a net gain of 3.1 dB. As power amplifier consume 25% of the total transceiver system power, a 3.1 dB net improvement in the efficiency of the PA of a mobile phone, for example, implies a

nearly 13% power saving of battery power. In addition, unlike other similar techniques, this improvement entails no additional system bandwidth.

A novel closed-form approximation for the BER of the proposed companding scheme is also presented in this paper. The accuracy of the proposed expression in comparison with the simulation is fully examined. Study cases have been included to cover the effect of companding on OFDM signal with and without an offset. The analysis presented in this work validates the proposed benefits of the ITMs scheme that will ultimately enhance the performance of many electronic products by lowering their power consumption in general, and reduce the charging frequency of the mobile counterparts in particular. In addition, the proper selection of the two companding and threshold parameters can be made in compliance with various design requirements of OFDM systems, hence making the system adaptive. The work has also been validated by a practical implementation of the proposed companding scheme using an FPGA platform.

## REFERENCES

- [1] S. Sen, R. Senguttuvan and A. Chatterjee, "Environment-Adaptive Concurrent Companding and Bias Control for Efficient Power-Amplification Operation," *IEEE Trans. Circuits and Syst.*, vol. 58, no. 3, pp 607-618, March 2011.
- [2] J. Armstrong, "Peak-to-average power reduction for OFDM by repeated clipping and frequency domain filtering," *Electronics Letters*, vol. 38, no. 5, pp. 246-247, Feb. 2002.
- [3] H. Ochiai and H. Imai, "On clipping for peak power reduction of OFDM signals," in *IEEE Global Communications Conference*, San Francisco, USA, pp. 731-735, Nov. 2000.
- [4] M. J. Hao and C. H. Lai, "Precoding for PAPR reduction of OFDM signals with minimum error probability," *IEEE Trans. Broadcasting*, vol. 56, no. 1, pp. 120-128, Mar. 2010.
- [5] Z. Taha and X. Liu, "An adaptive coding technique for PAPR reduction," in *IEEE Global Communications Conference*, Washington DC, USA, pp. 376-380, Nov. 2007.
- [6] D. Wu, "Selected mapping and partial transmit sequence schemes to reduce PAPR in OFDM systems," in *International Conference on Image Analysis and Signal Processing*, China, pp. 1-5, Oct. 2011.
- [7] J. C. Chen and C. P. Li, "Tone Reservation Using Near-Optimal Peak Reduction Tone Set Selection Algorithm for PAPR Reduction in OFDM Systems," *IEEE Signal Processing Letters*, vol. 17, pp. 933-936, Nov. 2010.
- [8] Y. Yang, Z. Zeng, S. Feng and C. Guo, "A Simple OFDM Scheme for VLC Systems Based on  $\mu$ -Law Mapping," *IEEE Photonics Technology Letters*, vol. 28, no. 6, pp. 641-644, March 2016.
- [9] M. Hu, Y. Li, W. Wang and H. Zhang, "A Piecewise Linear Companding Transform for PAPR Reduction of OFDM Signals With Companding Distortion Mitigation," *IEEE Trans. Broadcasting*, vol. 60, no. 3, pp. 532-539, Sept. 2014.
- [10] J. Hou, J.H. Ge, J. Li, "Trapezoidal companding scheme for peak-to-average power ratio reduction of OFDM signals," *Electronics Letters*, vol. 45, no. 25, pp. 1349-1351, Dec. 2009.
- [11] D. Lowe and X. Huang, "Optimal adaptive hyperbolic companding for OFDM," in *International Conference on Wireless Broadband and Ultra Wideband Communications*, Sydney, Australia, pp. 24-24, Aug. 2007.
- [12] Y. Wang, L. -H, Wang, J. -H. Ge, and B. Ai, "Nonlinear companding transform technique for reducing PAPR of OFDM signals," *IEEE Trans. Consumer Electronics*, vol. 58, no. 3, pp. 752-757, Aug. 2012.
- [13] X. Wang, T. Yihung, and C. Ng, "Reduction of peak-to-average power ratio of OFDM system using a companding technique," *IEEE Trans. Broadcasting*, vol. 45, no. 3, pp. 303-307, Sept. 1999.
- [14] Y. Wang, J. -H. Ge, L. -H. Wang, B. Ai, "Nonlinear Companding Transform Using Hyperbolic Tangent Function in OFDM Systems," in *International Conference on Wireless Communications, Networking and Mobile Computing*, China, pp. 1-4, Sept. 2012.

- [15] V. Tabatabavakili, A. Zahedi, "Reduction in peak to average power ratio of OFDM signals using a new Continuous Linear Companding Transform," in *International Symposium on Telecommunications*, Iran, pp. 426-430, Dec. 2010.
- [16] V. Yenamandra, L. Feiran, S. Al-Araji, N. Ali, M. Ismail, "Adaptive slope and threshold companding technique for PAPR reduction in OFDM systems," in *IEEE International Conference on Electronics, Circuits and Systems*, Seville, Spain, pp. 312-315, Dec. 2012.
- [17] R. Schmogrow, B. Nebendahl, M. Winter, A. Josten, D. Hillerkuss, S. Koenig, et al, "Error Vector Magnitude as a Performance Measure for Advanced Modulation Formats," *IEEE Photonics Technology Letters*, vol. 24, no. 1, pp.61-63, 2012.
- [18] T. G. Pratt, N. Jones, L. Smee, and M. Torrey, "OFDM Link Performance with Companding for PAPR Reduction in the Presence of Non-Linear Amplification," *IEEE Trans. Broadcasting*, vol. 52, no. 2, June 2006.
- [19] A. Goldsmith, *Wireless Communications*. Cambridge Univ. Press, 2005.

focused on the modeling, optimization, and control of time-varying dynamical systems, especially in computing and telecommunication settings. He has many articles published in peer reviewed high quality conferences and journals.



**Raed Abd-Alhameed** (M'06-SM'13) is a Professor of Electromagnetic and Radio Frequency (RF) Engineering in the School of Engineering, Design and Technology at the University of Bradford, UK. He has over 25 years research experience in RF designs, antennas, and electromagnetic computational techniques and has published over 400 academic Journals and referred conference papers. He has led several funded projects from the British Engineering and Physical Sciences Research Council (EPSRC), British Department of Trade and Industry (DTI), and the European Union.



**Nazar Ali** (M'01-SM'02) received the Ph.D. degree in Electrical and Electronic Engineering from the University of Bradford, UK, in 1990. From 1990 to 2000 he held various posts at the University of Bradford. He is currently an associate professor at Khalifa University in the United Arab Emirates. His current research interests include OFDM-based

systems, indoor and outdoor localization techniques and wearable antennas for medical applications.



**Rola Almahainy** (S'14) received the B.Sc. and MSc. degrees in Electrical and Computer Engineering from Khalifa University, United Arab Emirates (UAE), in 2013 and 2015, respectively. Currently, she is working as a teaching assistant at Khalifa University. Her research interests include multicarrier communication systems, broadcast technology and signal

processing.



**Abdullah Al-Shabali** (S'14) received the B.Sc. degree in electrical and electronic engineering in 2015 from Khalifa University and is currently pursuing the M.Sc. degree in electrical and computer engineering at the same University. His main technical interest are statistical signal processing and machine learning



**Nawaf Almoosa** (S'01-M'14) received his B.Sc. degree in Electronic Engineering from Khalifa University in 2004, and his M.Sc. and Ph.D. from the Georgia Institute of Technology in 2008 and 2014, respectively. His research interests span computer architecture, control theory and signal processing. His current work is